

## Fractal analysis of effective thermal conductivity for three-phase (unsaturated) porous media

Jianlong Kou,<sup>1,3</sup> Yang Liu,<sup>2</sup> Fengmin Wu,<sup>1,a)</sup> Jintu Fan,<sup>3,b)</sup> Hangjun Lu,<sup>1</sup> and Yousheng Xu<sup>1</sup>

<sup>1</sup>*Institute of Condensed Matter Physics, Zhejiang Normal University, Jinhua 321004, People's Republic of China*

<sup>2</sup>*Department of Mechanical Engineering, The Hong Kong Polytechnic University, Kowloon, Hong Kong, People's Republic of China*

<sup>3</sup>*Institute of Textiles and Clothing, The Hong Kong Polytechnic University, Kowloon, Hong Kong, People's Republic of China*

(Received 26 March 2009; accepted 18 July 2009; published online 4 September 2009)

A fractal analysis of effective thermal conductivity for unsaturated fractal porous media is presented based on the thermal-electrical analogy and statistical self-similarity of porous media. Here, we derive a dimensionless expression of effective thermal conductivity without any empirical constant. The effects of the parameters of fractal porous media on the dimensionless effective thermal conductivity are discussed. From this study, it is shown that, when the thermal conductivity of solid phase and wet phase are greater than that of the gas phase (viz.,  $k_s/k_g > 1$ ,  $k_w/k_g > 1$ ), the dimensionless effective thermal conductivity of unsaturated fractal porous media decreases with decreasing degree of saturation ( $S_w$ ) and increasing fractal dimension for pore area ( $D_f$ ), fractal dimension for tortuosity ( $D_t$ ), and porosity ( $\phi$ ); when the thermal conductivities of solid phase and wet phase are lower than that of the gas phase (viz.,  $k_s/k_g < 1$ ,  $k_w/k_g < 1$ ), the trends were just opposite. Our model was validated by comparing the model prediction with existing experimental data. Excellent agreement was found except for the cases at very low level of saturation. © 2009 American Institute of Physics. [doi:10.1063/1.3204479]

### I. INTRODUCTION

As a transport property, effective thermal conductivity of porous media has received much attention due to its wide applications in many fields, including chemical engineering, soil science, engineering, oil production, polymer composite molding, etc. The microstructures of porous media are usually disordered and extremely complicated in nature, which makes it very difficult to obtain an analytical expression for the thermal conductivity, especially for the natural unsaturated (or multiphase) porous media.

In the past, the thermal conductivity of porous media has been studied by many investigators<sup>1-8</sup> through different approaches, including numerical solutions, theoretical approaches, and experiments. Nozad *et al.*<sup>9</sup> used transient method to determine effective thermal conductivities for two phase and extended to three-phase systems. They made an experimental investigation with three fluids (air, glycerol, and water) and five solids (glass, stainless steel, bronze, urea formaldehyde, and aluminum). They found that the measured values of the effective thermal conductivity for three-phase systems were generally higher than the theoretical values. Singh *et al.*<sup>10</sup> performed an experimental investigation by using dune sand and brick sandsamples to determine the thermal conductivity of three-phase (unsaturated) porous media. They tested different types of soils saturated with different liquids having variations in liquid content and temperature. Zhang *et al.*<sup>11</sup> applied a randomly mixed model to

calculate the effective thermal conductivity of a multiphase system. The model was based on the assumption that the smallest part of the phases is a cube, and all the cubes were randomly dispersed in the space. The effective thermal conductivity was calculated numerically from thermal conductivities and volume fractions of the components, using the principle of heat conduction in anisotropic media. The prediction did not depend on empirical parameters and the algorithm was easy to perform in a personal computer. The model was validated by several types of moist porous media with various porosities and degrees of the degree of saturation. Vermats *et al.*<sup>12</sup> conducted an experimental investigation to determine the thermal conductivity of three-phase unsaturated porous media with differential temperature sensor method. Their results were in good agreement with the values predicted by the geometry dependent resistor model developed for the three-phase system.

The porous media have been proven to be fractal objects in nature.<sup>13-18</sup> This means that the fractal theory may be used to predict properties of porous media. Yu and Cheng<sup>19</sup> developed a fractal thermal conductivity model for bidispersed (saturated) porous media based on the fractal characteristics of unit cell of the media, and this fractal model is also applicable for analyzing the permeability of porous media. Although Yu's model does not contain any empirical constant and good agreement was found between the model predictions and experimental data, it is not applicable to unsaturated porous media. The saturated porous medium is, in fact, only the special case of the unsaturated porous medium. It is therefore meaningful to develop an analytical solution for the thermal conductivity of unsaturated (or multiphase) porous

<sup>a)</sup>Electronic mail: wfm@zjnu.cn.

<sup>b)</sup>Electronic mail: tcfanjt@inet.polyu.edu.hk.

media. With one-dimensional heat flow assumption, Ma *et al.*<sup>20</sup> derived a fractal geometry model for the effective thermal conductivity of three-phase unsaturated porous media based on the method of thermal-electrical analogy and exact self-similar Sierpinski carpet. The effective thermal conductivity of fractal geometry model was expressed as a function of porosity (related to stage  $n$  of Sierpinski carpet), ratio of areas, ratio of component thermal conductivities, and the degree of saturation. However, Ma's model has an important practical limitation, as it only applies to exactly self-similar porous media, yet real porous media, like many objects found in nature, are not exactly self-similar, but statistically self-similar. Such a statistically self-similar porous media can be called as the fractal porous media.

The objective of the present work is to develop an analytical method and a fractal model for predicting the effective thermal conductivity of three-phase (unsaturated) porous media based on the available evidence that porous media in nature are fractal objects.<sup>13–18</sup> In Sec. II, we give the detailed description of the fractal characteristics of microstructures of fractal porous media, and in Sec. III, we present fractal analysis of effective thermal conductivity for three-phase (unsaturated) porous media. Results and discussion are presented in Sec. IV. Lastly, some concluding remarks are given in Sec. V.

## II. THE FRACTAL DESCRIPTION OF POROUS MEDIA

An object measurement is related to its dimension and is invariant with the unit of measurement used. In general, ordered objects such as points, lines, surfaces and cubes can be described by Euclidean geometry using integer dimension 0, 1, 2 and 3, respectively. However, it is found that numerous objects are irregular and disordered in nature such as rough surfaces, mountains, coastlines, lakes, rivers and islands. They can not use the Euclidean description. These objects are called fractals, and the dimensions of such objects are non-integral and defined as fractal dimensions. The measure of a fractal object  $M(L)$  is related to the length scale  $L$  by the following scaling law form<sup>21</sup>

$$M(L) \sim L^{D_f}, \quad (1)$$

where  $M$  can be the length of a line or the area of a surface or the volume of a cube or the mass of an object and  $D_f$  is the fractal dimension of an object. In fractal geometry, there are two kinds of self-similar sets: one is exactly self-similar fractals such as Sierpinski carpet, Sierpinski gasket, and Koch curve, the other is statistically self-similar such as real porous medium. Exact self-similar fractals are rare in nature. It has been shown that the size distribution of pores in porous media follows the fractal power law,<sup>18,22</sup>

$$N(L \geq \lambda_{\min}) = \left( \frac{\lambda_{\max}}{\lambda} \right)^{D_f}, \quad (2)$$

where  $D_f$  is the pore area fractal dimension,  $0 < D_f < 2$  in two dimensions, and  $\lambda$ ,  $\lambda_{\min}$ , and  $\lambda_{\max}$  are the pore size, minimum pore size, and maximum pore size, respectively. Differentiating Eq. (2) with respect to  $\lambda$  results in the number

of pores whose sizes are within the infinitesimal range  $\lambda$  to  $\lambda + d\lambda$ ,<sup>22</sup>

$$-dN = D_f \lambda_{\max}^{D_f} \lambda^{-(1+D_f)} d\lambda. \quad (3)$$

The negative sign in Eq. (3) expresses that the island or pore number decreases with the increase in island or pore size and  $-dN > 0$ . Equation (3) describes the scaling relationship of the cumulative pore population. The total number of pores or islands from the smallest diameter  $\lambda_{\min}$  to the largest diameter  $\lambda_{\max}$ , can be obtained from Eq. (2) as<sup>24</sup>

$$N_t(L \geq \lambda_{\min}) = \left( \frac{\lambda_{\max}}{\lambda_{\min}} \right)^{D_f}. \quad (4)$$

Dividing Eq. (3) by Eq. (4) gives

$$-\frac{dN}{N_t} = D_f \lambda_{\min}^{D_f} \lambda^{-(1+D_f)} d\lambda = f(\lambda) d\lambda, \quad (5)$$

where  $f(\lambda) = D_f \lambda_{\min}^{D_f} \lambda^{-(1+D_f)} \geq 0$  is the probability density function and the pore area fractal dimension  $D_f$  is determined by<sup>18</sup>

$$D_f = d + \frac{\ln \phi}{\ln \frac{\lambda_{\max}}{\lambda_{\min}}}, \quad (6)$$

where  $d$  is the Euclidean dimension and  $d=2$  and  $3$  represents the two and three dimensional spaces, respectively. With probability theory, the probability density function  $f(\lambda)$  should satisfy the following relationship<sup>24</sup>:

$$\int_0^\infty f(\lambda) d\lambda = \int_{\lambda_{\min}}^{\lambda_{\max}} f(\lambda) d\lambda = 1 - \left( \frac{\lambda_{\min}}{\lambda_{\max}} \right)^{D_f} \equiv 1. \quad (7)$$

It is clear that Eq. (7) holds if and only if<sup>22</sup>

$$\frac{\lambda_{\min}}{\lambda_{\max}} \equiv 0 \quad (8)$$

is satisfied. Equation (8) implies that  $\lambda_{\min} \ll \lambda_{\max}$  must be satisfied for fractal analysis of porous media, otherwise the porous media are nonfractal media. For example, if  $\lambda_{\min} = \lambda_{\max}$ , Eqs. (6)–(8) do not hold. Equation (8) can thus be considered as a criterion to judge whether a porous media can be characterized by the fractal theory and technique. This means that if Eq. (8) does not hold, the porous media are nonfractal media, and the fractal theory and technique are not applicable to the media. Fortunately, in general,  $\lambda_{\min}/\lambda_{\max} = 10^{-2}$  or  $< 10^{-2}$  in porous media, thus Eq. (8) holds for porous media.<sup>24</sup> Thus, the fractal theory and technique can be used to analyze the characters of porous media.

A porous media having various pore sizes that can be considered as a bundle of tortuous capillary tubes with variable cross sectional areas, with diameter and tortuous length (actual length) being  $\lambda$  and  $L_t(\lambda)$ , respectively. Due to the tortuous nature of capillary, the tortuous length  $L_t(\lambda)$  is greater than or equal to the straight length  $L_0$ . Wheatcraft and Tyler<sup>23</sup> showed that a fractal path travelled of a particle through a heterogeneous porous medium can be described as  $L_t(\varepsilon) = \varepsilon^{1-D_f} L_0^{D_f}$  [where  $L_t(\varepsilon)$  is the actual length and the  $\varepsilon$  is the pore size]. Based on this, Yu *et al.*<sup>24</sup> argued that the

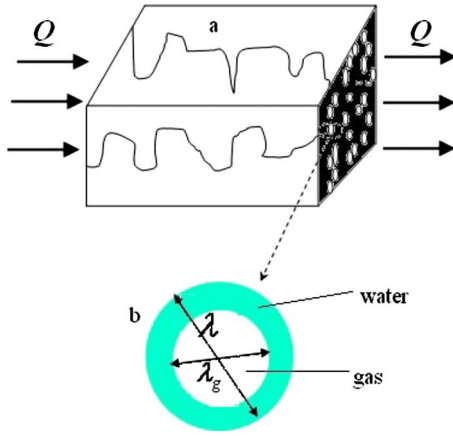


FIG. 1. (Color online) (a) A schematic diagram of porous media for heat transfer and (b) a schematic of the cross section of porous media filled with wetting phase (water) and nonwetting phase (gas).

diameter of capillaries is analogous to the length scale  $\varepsilon$  and extended the fractal scaling relationship between the diameter and length of capillaries,

$$L_t(\lambda) = \lambda^{1-D_t} L_0^{D_t}, \quad (9)$$

where  $1 < D_t < 2$  is the fractal dimension for tortuosity in two dimensions.  $D_t=1$  represents a straight capillary, a higher value of  $D_t$  corresponds to a highly tortuous capillary, and  $D_t=2$  corresponds to a highly tortuous line that fills whole space.

On the basis of the porous media characteristics, the thermal conductivity of porous media can be expressed in terms of an aggregation of parallel and serial layers consisting of solid (s), water (w), and gas (g) (see Fig. 1). The pores in a cross section can be considered as circles with different diameters  $\lambda$ ,<sup>26</sup> a simplified model for the cross section of a capillary tube partially filled with water and gas as shown in Fig. 1(b). The total pore area in the cross section  $A_p$  can be obtained as

$$A_p = - \int_{\lambda_{\min}}^{\lambda_{\max}} \pi(\lambda/2)^2 dN = \frac{\pi D_f \lambda_{\max}(1-\phi)}{4(2-D_f)}. \quad (10)$$

So the total cross sectional area  $A$  can be obtained as

$$A = \frac{A_p}{\phi} = \frac{\pi D_f \lambda_{\max}(1-\phi)}{4(2-D_f)\phi}, \quad (11)$$

where  $\phi$  is the effective porosity of porous media. The frontal part presents a complete description of the fractal characters of porous media and our fractal porous media model.

### III. EFFECTIVE THERMAL CONDUCTIVITY FOR UNSATURATED POROUS MEDIA

In this section, the effective thermal conductivity is derived based on the thermal-electrical analogy. Under the assumption of one-dimensional heat flow, the thermal-electrical analogy technique had been successfully applied to analyze the effective thermal conductivity of heterogeneous media such as porous media by many researchers.<sup>3,19,20</sup> According to the Fourier's law, the thermal resistance of a single channel  $r$  can be expressed as

$$r(\lambda) = \frac{L_t(\lambda)}{A(\lambda)k} = \frac{4L_t(\lambda)}{\pi\lambda^2k}, \quad (12)$$

where the  $k$  is thermal conductivity. The thermal resistance of a single channel of the nonwetting phase (or gas)  $r_g$  can be expressed as

$$r_g = \frac{4L_t(\lambda)}{\pi\lambda^2k_g}, \quad (13)$$

where the  $k_g$  is the thermal conductivity of nonwetting phase. The thermal resistance of the nonwetting phase (or gas)  $r_g$  can be considered to be in parallel. In the interval of  $\lambda$  and  $\lambda+d\lambda$ , there are  $(-dN)$  parallel pores that satisfy Eq. (3). The thermal resistance of a pore is  $-dN/r_g$  and the total thermal resistance ( $R_g$ ) of nonwetting phase can be expressed as<sup>25,26</sup>

$$\frac{1}{R_g} = - \int_{\lambda_{\min,g}}^{\lambda_{\max,g}} \frac{1}{r_g} dN = - \int_{\lambda_{\min,g}}^{\lambda_{\max,g}} \frac{\pi\lambda^2k_g}{4L_t(\lambda)} dN. \quad (14)$$

Inserting Eqs. (3) and (9) into Eq. (14), we obtain the thermal resistance of nonwetting phase of porous media as follow:

$$R_g = \frac{4L_0^{D_t}(D_t - D_{f,g} + 1)}{\pi k_g D_{f,g} \lambda_{\max,g}^{D_t+1} [1 - (\lambda_{\min,g}/\lambda_{\max,g})^{D_t-D_{f,g}+1}]}, \quad (15)$$

where  $\lambda_{\max,g}$  and  $\lambda_{\min,g}$  are the maximum and minimum equivalent diameters of the pores in nonwetting phase (such gas) and  $D_{f,g}$  is the fractal dimension for nonwetting phase in porous media,  $1 < D_{f,g} < 2$  in two dimensions. These expressions are<sup>27</sup>

$$\lambda_{\max,g} = \lambda_{\max} \sqrt{1 - S_w}, \quad (16)$$

$$\lambda_{\min,g} = \lambda_{\min} \sqrt{1 - S_w}, \quad (17)$$

$$D_{f,g} = 2 + \frac{\ln[(1 - S_w)\phi]}{\ln \frac{\lambda_{\max}}{\lambda_{\min}}} = 2 - \frac{\ln[(1 - S_w)\phi]}{\ln \frac{\lambda_{\min} \sqrt{1 - S_w}}{\lambda_{\max} \sqrt{1 - S_w}}} = 2 - \frac{\ln \phi_w}{\ln \frac{\lambda_{\min,g}}{\lambda_{\max,g}}}, \quad (18)$$

where  $S_w$  and  $\phi_w$  are the degree of saturation and ratio of the wetting phase, respectively.

Similarly, the thermal resistance expression for the wetting phase (or water) phase in unsaturated porous medium can be obtained as

$$R_w = \frac{4L_0^{D_t}(D_t - D_{f,w} + 1)}{\pi k_w D_{f,w} \lambda_{\max,w}^{D_t+1} [1 - (\lambda_{\min,w}/\lambda_{\max,w})^{D_t-D_{f,w}+1}]}, \quad (19)$$

where the  $k_w$  is the thermal conductivity of the wetting phase,  $\lambda_{\max,w}$  and  $\lambda_{\min,w}$  are the largest and the minimum equivalent diameter for wetting phase (such water), and  $D_{f,w}$  is the fractal dimension for wetting phase in porous media and  $1 < D_{f,w} < 2$  in two dimensions. These expressions are<sup>27</sup>

$$\lambda_{\max,w} = \lambda_{\max} \sqrt{S_w}, \quad (20)$$

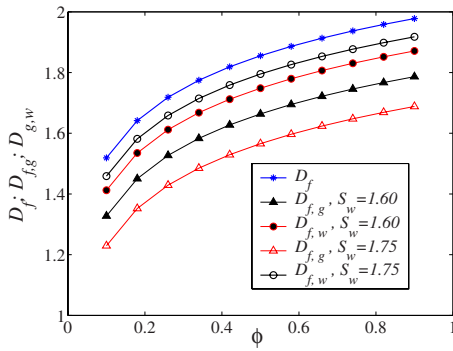


FIG. 2. (Color online) Fractal dimension: pore area fractal dimension  $D_f$ , gas (nonwetting) phase fractal dimension  $D_{f,g}$ , and water (wetting) phase fractal dimension  $D_{f,w}$  vs porosity under different degrees of saturations.

$$\lambda_{\min,w} = \lambda_{\min} \sqrt{S_w}, \tag{21}$$

$$D_{f,w} = 2 + \frac{\ln[S_w \phi]}{\ln \frac{\lambda_{\max}}{\lambda_{\min}}} = 2 - \frac{\ln[S_w \phi]}{\ln \frac{\lambda_{\min} \sqrt{S_w}}{\lambda_{\max} \sqrt{S_w}}} = 2 - \frac{\ln \phi_w}{\ln \frac{\lambda_{\min,w}}{\lambda_{\max,w}}}. \tag{22}$$

For the solid phase of porous media, the thermal resistance ( $R_s$ ) can be obtained as

$$R_s = \frac{L_0}{(1 - \phi) A k_s}. \tag{23}$$

The effective thermal conductivity of the porous media ( $k_e$ ) can be expressed as

$$k_e = \frac{1}{R_t} \frac{L_0}{A} = \frac{L_0}{A} \left( \frac{1}{R_g} + \frac{1}{R_w} + \frac{1}{R_s} \right), \tag{24}$$

where  $R_t$  is total thermal resistance.

Inserting Eqs. (11), (15), (19), and (23) into Eq. (24), the dimensionless effective thermal conductivity of porous medium can be expressed as

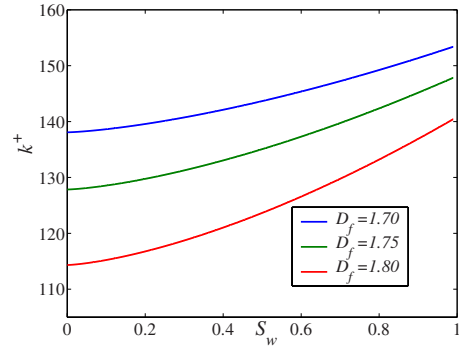


FIG. 4. (Color online) Dimensionless effective thermal conductivity vs the degree of saturations at different fractal dimensions  $D_f$ .

$$k^+ = \frac{k_e}{k_g} = \frac{D_{f,g}(2 - D_f) \phi \lambda_{\max,g}^{D_f+1} [1 - (\lambda_{\min,g}/\lambda_{\max,g})^{D_t - D_{f,g} + 1}]}{D_f L_0^{D_f-1} \lambda_{\max}^2 (D_t - D_{f,g} + 1)(1 - \phi)} + \frac{D_{f,w}(2 - D_f) \phi \lambda_{\max,w}^{D_f+1} [1 - (\lambda_{\min,w}/\lambda_{\max,w})^{D_t - D_{f,w} + 1}] k_w}{D_f L_0^{D_f-1} \lambda_{\max}^2 (D_t - D_{f,w} + 1)(1 - \phi) k_g} + (1 - \phi) \frac{k_s}{k_g}. \tag{25}$$

It is evident that the dimensionless thermal conductivity  $k^+$  is a function of the degree of saturation  $S_w$ , fractal dimensions  $D_f$ ,  $D_t$ , and  $D_{f,w}$  (or  $D_{f,g}$ ), and there is not any empirical constant in this fractal thermal conductivity model.

#### IV. RESULTS AND DISCUSSION

Figure 2 plots the pore area fractal dimension  $D_f$ , the phase fractal dimensions  $D_{f,g}$  and  $D_{f,w}$  versus the porosity  $\phi$  at different degrees of saturations  $S_w$ . It is seen from Fig. 2 that the pore area fractal dimension  $D_f$ , and the phase fractal dimensions  $D_{f,g}$  and  $D_{f,w}$  increase with porosity  $\phi$ , and as porosity approaches to 1, the fractal dimension  $D_f$  is close to 2. This is understandable as higher porosity implies larger pore area, which leads to higher fractal dimension. In the special case of porosity approaching to 1, the unit cell of the media becomes completely void, which has the fractal dimension of 2. Another important phenomenon, which can be observed from Fig. 2, is that the curve of the wetting phase is close to the curve of the pore area fractal dimension, and the curve of the nonwetting phase (such gas) reaches the maxi-

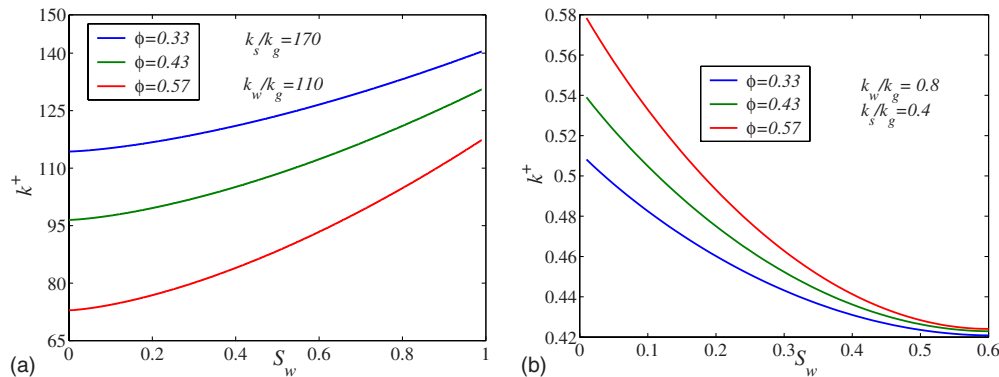


FIG. 3. (Color online) Dimensionless effective thermal conductivity of the present model vs saturation in different porosities and  $k_s/k_g$ ,  $k_w/k_g$ .



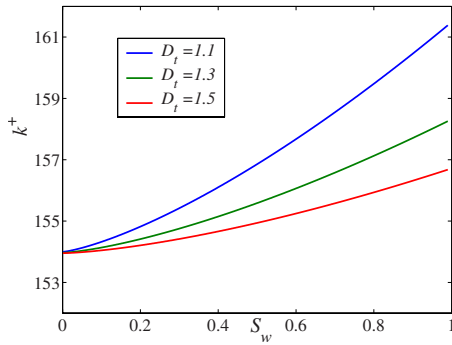


FIG. 5. (Color online) Dimensionless effective thermal conductivity vs the degree of saturation at different fractal dimensions for tortuosity  $D_t$ .

imum value of 1 as the degree of saturation increases. It should be noted that as the degree of saturation approaches to zero, viz., the media are fully filled with a nonwetting fluid (i.e., gas), the fractal dimension becomes exactly the same as that for the saturated porous medium. One interpretation for this is that, higher the degree of saturation implies larger proportion of wetting phase, leading to higher fractal dimension  $D_{f,w}$ , the same is true for fractal dimension  $D_{f,g}$ .

Figure 3 plots the dimensionless thermal conductivity against the degree of saturation under different porosities. From Fig. 3(a), we can see that the thermal conductivity increases as the porosity decreases when  $k_s/k_g > 1$  and  $k_w/k_g > 1$ . This can be explained by the fact that a higher porosity implies smaller solid volume fraction of higher thermal conductivity, leading to a reduction in the effective thermal conductivity. However, it is found that, when  $k_s/k_g < 1$  and  $k_w/k_g < 1$ , the opposite phenomenon is observed, the thermal conductivity increases with the increase in porosity. The reason is that when  $k_s/k_g < 1$  and  $k_w/k_g < 1$ , the matrix space having higher thermal conductivity dominates the effective thermal conductivity, resulting in a higher effective thermal conductivity at a higher porosity.

Figure 4 plots the dimensionless effective thermal conductivity  $k^+$  versus the degree of saturation at different pore area fractal dimensions  $D_f$  and at a given tortuosity fractal dimension  $D_t = 1.1$ . It is seen that the effective thermal conductivity increases with the increase in the degree of saturation at  $k_s/k_g = 167.5$ ,  $k_w/k_g = 110$ , and fixed tortuosity fractal dimension  $D_t$ . This can be explained as, when the degree of saturation increases, the wetting (water) phase volume frac-

TABLE I. The experimental conditions (Refs. 10 and 20) of Nonwetting (gas)  $k_g = 0.02 \text{ W m}^{-1} \text{ K}^{-1}$  and wetting (water)  $k_w = 2.2 \text{ W m}^{-1} \text{ K}^{-1}$ , at temperature of  $20^\circ \text{C}$ , and here  $k_e^+ = k_e/k_g$ .

	Saturation $S_w$	$k_e$ ( $\text{W m}^{-1} \text{ K}^{-1}$ )	$k_e^+$ ( $\text{W m}^{-1} \text{ K}^{-1}$ )
$k_s = 3.35 \text{ W m}^{-1} \text{ K}^{-1}$	0.00	0.176	8.80
	0.03	0.294	14.70
	0.23	0.752	37.60
	0.52	1.137	56.85
	0.72	1.438	71.90
$k_s = 2.85 \text{ W m}^{-1} \text{ K}^{-1}$	0.00	0.12	6.00
	0.08	0.36	18.00
	0.22	0.50	25.00
	0.46	0.71	35.50
	0.63	0.92	46.00

tion with higher thermal conductivity increases, leading to the increase in the effective thermal conductivity. It can also be observed that the thermal conductivity decreases as  $D_f$  increases. This is understandable as porosity increases with the increase of  $D_f$  and higher porosity leads to the reduction in thermal conductivity.

The effect of fractal dimensions of tortuosity on the dimensionless thermal conductivity is further investigated. Figure 5 plots the dimensionless thermal conductivity versus the degree of saturation at different tortuous fractal dimensions  $D_t$  and at given pore area fractal dimensions  $D_f = 1.7$ . From Fig. 5, it can be shown that the thermal conductivity decreases with increasing tortuosity fractal dimensions  $D_t$ . The decrease in thermal conductivity with the increase in  $D_t$  is attributed to the increased heat resistance due to the higher the tortuosity dimension. The higher the tortuosity dimension implies longer distance of heat transport through more tortuous channels, leading to the increase in resistance and the decrease in the effective thermal conductivity.

Figure 6 compares the present model predictions of thermal conductivity of  $k_s = 3.35$  and  $k_s = 2.85 \text{ W m}^{-1} \text{ K}^{-1}$  with the available experimental data<sup>10</sup> reported in Table I. In general, very good agreement is found between the present model predictions and the available experimental data, except for the data at the very low degree of saturation.

Figure 7 compares the predictions of the present model with the more recent experimental data by Kohout.<sup>28</sup> The

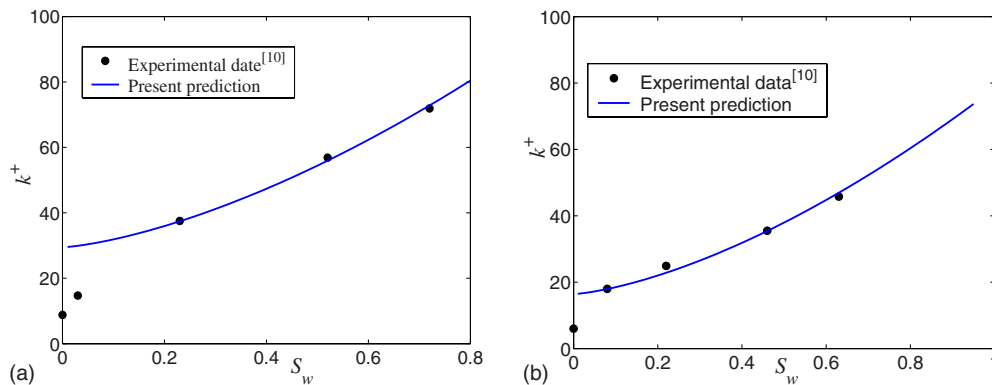


FIG. 6. (Color online) Comparison between the model prediction and existing experimental data.

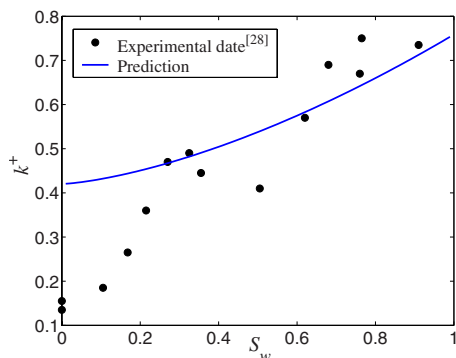


FIG. 7. (Color online) Comparison between the model prediction and existing experimental data.

experimental parameters are  $k_s=0.8 \text{ W m}^{-1} \text{ K}^{-1}$ ,  $k_w=0.61 \text{ W m}^{-1} \text{ K}^{-1}$ , and  $k_g=0.025 \text{ W m}^{-1} \text{ K}^{-1}$ . Again, there is very good agreement between the model prediction and the experimental data, when  $S_w$  is larger than 0.2. The greater discrepancy at the low level of saturation may be due to the fact that at the low saturation, majority of the water is not in the free form, but absorbed by the solid materials.<sup>29–32</sup> Nevertheless, the present model treats the wet phase and solid phase separately, i.e., no moisture sorption or desorption takes place.

Although, the general relationship between the thermal conductivity and the parameters of the fractal porous media has been established in the present model, it must be noted that the model is derived under a number of assumptions, including one dimensional heat flow, no sorption or desorption, no phase change, and no flow of gas phase and wetting phase. Heat flow in real porous media may be more complex,<sup>29–32</sup> involving multidimensional heat flow, phase change, flow of wetting phase and gas phase, etc. The micro- or nanostructures of the solid phase may also have significant effects.

## V. CONCLUSIONS

In this paper, based on the assumption of one-dimensional heat transfer, we derived a steady state fractal model for the prediction of thermal conductivity of unsaturated porous media by applying thermal-electrical analogy and statistical self-similarity. We first defined a dimensionless effective thermal conductivity of unsaturated fractal porous media and investigated the relationship between the dimensionless effective thermal conductivity and the geometrical parameters of the unsaturated fractal porous media. From this investigation, it is shown that, when the thermal conductivity of solid phase and wet phase are greater than that of the gas phase (viz.,  $k_s/k_g > 1$ ,  $k_w/k_g > 1$ ), the dimensionless effective thermal conductivity of unsaturated fractal porous media decreases with decreasing degree of saturation ( $S_w$ ) and increasing fractal dimension for pore area ( $D_f$ ), fractal dimension for tortuosity ( $D_t$ ), and porosity ( $\phi$ );

when the thermal conductivities of solid phase and wet phase are lower than that of the gas phase (viz.,  $k_s/k_g < 1$ ,  $k_w/k_g < 1$ ), the trends were just opposite. The predictions of the model are compared with available experimental data and showed very good agreement except for the cases at low level of saturation, at which majority of the wetting phase may be absorbed by the solid phase.

## ACKNOWLEDGMENTS

The author would like to thank Professor Boming Yu for many helpful discussions and comments. This work was partially supported by the the State Key Development Project for Basic Research of China (Grant No. 2006CB708612), the National Natural Science Foundation of China Grant (No. 10572130), the Natural Science Foundation of Zhejiang Province, China (Grant No. Y607425), and Hong Kong Polytechnic University Niche Area Project (Project No. 1-BB82).

- <sup>1</sup>W. Woodside and J. H. Messmer, *J. Appl. Phys.* **32**, 1699 (1961).
- <sup>2</sup>L. S. Verma, A. K. Shrotriya, R. Singh, and D. R. Chaudhary, *J. Phys. D* **24**, 1729 (1991).
- <sup>3</sup>C. T. Hus, P. Cheng, and K. W. Wong, *J. Heat Transfer* **117**, 264 (1995).
- <sup>4</sup>K. J. Singh, R. Singh, and D. R. Chaudhary, *J. Phys. D* **31**, 1681 (1998).
- <sup>5</sup>R. J. Goldstein, W. E. Ibele, S. V. Patankar, T. W. Simon, T. H. Kuehn, P. J. Strykowski, K. K. Tamma, J. V. R. Heberlein, J. H. Davidson, J. Bischof, F. A. Kulacki, U. Kortshagen, S. Garrick, and V. Srinivasan, *Int. J. Heat Mass Transfer* **49**, 451 (2006).
- <sup>6</sup>J. G. Berryman, *Appl. Phys. Lett.* **86**, 032905 (2005).
- <sup>7</sup>H. F. Zhang, X. S. Ge, and H. Ye, *Appl. Phys. Lett.* **89**, 081908 (2006).
- <sup>8</sup>M. R. Wang and N. Pan, *Int. J. Heat Mass Transfer* **51**, 1325 (2008).
- <sup>9</sup>I. Nozad, R. G. Carbonell, and S. Whitaker, *Chem. Eng. Sci.* **40**, 857 (1985).
- <sup>10</sup>A. K. Singh, R. Singh, and D. R. Chaudhary, *J. Phys. D* **23**, 698 (1990).
- <sup>11</sup>H. F. Zhang, X. S. Ge, and H. Ye, *J. Phys. D* **39**, 220 (2006).
- <sup>12</sup>L. S. Verma, A. K. Shrotriya, Ramvir Singh, and D. R. Chaudhary, *J. Phys. D* **24**, 1515 (1991).
- <sup>13</sup>A. J. Katz and A. H. Thompson, *Phys. Rev. Lett.* **54**, 1325 (1985).
- <sup>14</sup>C. E. Krohn and A. H. Thompson, *Phys. Rev. B* **33**, 6366 (1986).
- <sup>15</sup>I. M. Young and J. W. Crawford, *J. Soil Sci.* **42**, 187 (1991).
- <sup>16</sup>J. M. Smidt and D. M. Monro, *Fractals* **6**, 401 (1998).
- <sup>17</sup>B. M. Yu, L. J. Lee, and H. Q. Cao, *Fractals* **9**, 155 (2001).
- <sup>18</sup>B. M. Yu and J. H. Li, *Fractals* **9**, 365 (2001).
- <sup>19</sup>B. M. Yu and P. Cheng, *J. Thermophys. Heat Transfer* **16**, 22 (2002).
- <sup>20</sup>Y. T. Ma, B. M. Yu, D. M. Zhang, and M. Q. Zou, *J. Appl. Phys.* **95**, 6426 (2004).
- <sup>21</sup>B. B. Mandelbrot, *The Fractal Geometry of Nature* (W. H. Freeman, New York, 1982).
- <sup>22</sup>B. M. Yu, *Appl. Mech. Rev.* **61**, 050801 (2008).
- <sup>23</sup>S. W. Wheatcraft and S. W. Tyler, *Water Resour. Res.* **24**, 566 (1988).
- <sup>24</sup>B. M. Yu and P. Cheng, *Int. J. Heat Mass Transfer* **45**, 2983 (2002).
- <sup>25</sup>B. M. Yu and W. Liu, *AIChE J.* **50**, 46 (2004).
- <sup>26</sup>B. M. Yu, J. H. Li, Z. H. Li, and M. Q. Zou, *Int. J. Multiphase Flow* **29**, 1625 (2003).
- <sup>27</sup>B. M. Yu and J. H. Li, *Fractals* **12**, 17 (2004).
- <sup>28</sup>M. Kohout, A. P. Collier, and F. Stepanek, *Int. J. Heat Mass Transfer* **47**, 5565 (2004).
- <sup>29</sup>E. Y. B. Li and J. Fan, *Numer. Heat Transfer, Part A* **51**, 635 (2007).
- <sup>30</sup>J. Fan and X. Cheng, *Text. Res. J.* **75**, 187 (2005).
- <sup>31</sup>X. Cheng and J. Fan, *Int. J. Therm. Sci.* **43**, 665 (2004).
- <sup>32</sup>J. Fan, X. Cheng, X. Wen, and W. Sun, *Int. J. Heat Mass Transfer* **47**, 2343 (2004).